Thermo-mechanical design and birefringence analysis for the MezzoCielo assembly

Silvio Di Rosa[a,*], Roberto Ragazzoni[a,b], Marco Dima[b], Luigi Lessio[b], Carmelo Arcidiacono[b], Demetrio Magrin[b], Jacopo Farinato[b], and Simone Zaggia[b]

[a]University of Padua, Department of Physics and Astronomy, Vicolo dell'Osservatorio 5, Padua, Italy, 35122
[b]Italian Institute for Astrophysics (INAF), Vicolo dell'Osservatorio 5, Padua, Italy, 35122

ABSTRACT

MezzoCielo represents a novel type of monocentric optical instrument devoted to whole-sky monitoring due to its extremely large field of view. The latter property, combined with the need to realize relative wide optical spheres (with diameters up to few meters) and the limitations related to the manufacturing of large optical elements having high performance, requires the adoption of a segmented structure, presenting, for instance, a Platonic solid-like shape, composed by several identical lenses, supported by a metallic frame along the edges of the solid itself. In this paper, the main aspects concerning the sizing of such frame (chosen to be dodecahedral) and a thermo-mechanical analysis of the lenses support assembly, both analytical and numerical, will be presented. In particular, it will be shown how the lenses are able to operate with little temperature difference across their volume independently from the surrounding conditions and the way in which the telescope can withstand external low temperatures without manifesting high thermal stresses, while maintaining, at the same time, constant focal length. Subsequently, a birefringence investigation completes the opto-mechanical analysis and it will be employed as a further instrument to select the more appropriate lens shape. Eventually, the same analysis is repeated for all the twelve lenses of the dodecahedral structure.

Keywords: Large Telescopes, Monocentric Systems, Thermo-mechanical Sizing, Birefringence, Optical Fluids

1. INTRODUCTION

MezzoCielo is a novel concept of global field of view optical instruments, conceived with the aim of simultaneously surveying the whole sky observable from a single site on Earth. For this purpose, it employs 1-m aperture lenses arranged upon the faces of a dodecahedral structure, realized in order to provide the telescope a spherical symmetry. Optically, the device is a monocentric system, constituted by a BK7 glass shell, encompassing a proper optical fluid, required in order to make the telescope actually convergent with relatively high focal ratio (greater than 3).[1] In Ref. 2, a complete optical characterization of two promising optical fluids is reported. Here, the most dense fluid, the perfluorohexane FC-72, is employed for the quantification of the hydrostatic loads acting upon the lenses.

For a dodecahedral configuration, previous studies[3] have analytically shown that, in order to achieve a maximum glass deflection of 20 μm, the circular simply supported lens of the assembly, made of BK7, analyzed under the hypothesis of thin plate theory[4] must present a thickness of at least 120 mm for a 2000 mm diameter sphere. Finite Elements Analysis (FEA) have actually demonstrated that, for such configuration, the maximum displacement at the lens center is around 10 μm: indeed, the analytical estimation slightly over-sizes stresses and strains since the thin plate theory does not consider the actual geometry of the meniscus lens, nor stresses and strains along the axis normal to the lens plane. These results, in particular, have been obtained for the lowermost lens of the telescope, located at the bottom of the structure and, as such, subjected to the highest hydrostatic loads.

Given these premises, it is chosen to consider, as the sizing starting point, a dodecahedron inscribed in a 1120 mm radius sphere, comprising 12 identical meniscus BK7 lenses 120 mm thick with clear aperture of 1000 mm each, enclosing a 1000 mm radius sphere filled with FC-72 fluid. A representation of the assembly is given in

Advances in Optical and Mechanical Technologies for Telescopes and Instrumentation VI, edited by Ramón Navarro, Ralf Jedamzik, Proc. of SPIE Vol. 13100, 131004V
 · 0277-786X · doi: 10.1117/12.3020197

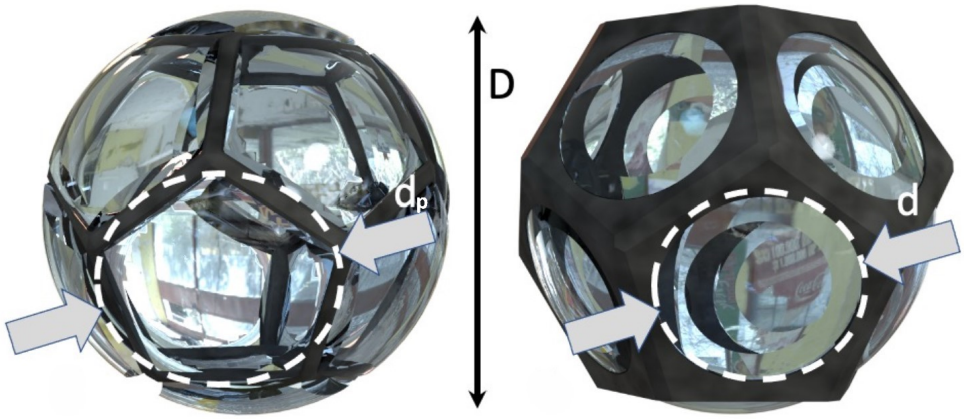

(a) (b)

Figure 1. Realistic representation of the telescope assembly. Since the instrument is, geometrically, a dodecahedron, the lenses could be either pentagonal or circular: (a) pentagonal shape lenses, (b) circular shape lenses. For a given overall diameter D, the parameters denoted in figure with d_p and d are related by the relation $d_p \approx 1.24d$

fig. 1. Since we are dealing with a dodecahedron, the lenses could have either a pentagonal shape or a circular one. In both cases, the supporting frame must occupy the edges of the pentagonal faces. In this work, the thermo-mechanical behaviour of both configurations have been investigated.

2. THERMO-MECHANICAL SIZING

The starting point of the thermal sizing is the quantification of the telescope focal length. For a monocentric lens, the latter can be written as:

$$f = \frac{R_1 R_2 n_1 n_2}{2(n_1 - 1)R_2 n_2 + 2(n_2 - n_1)R_1}, \tag{1}$$

with R_1 and R_2 telescope outer and inner radius respectively and n_1 and n_2 refractive indices of BK7 and FC-72 respectively. The uncertainty associated with the focal length, Δf, can instead be estimated from the propagation of uncertainties:

$$\Delta f = \sqrt{\left(\frac{df}{dR_1}\Delta R_1\right)^2 + \left(\frac{df}{dR_2}\Delta R_2\right)^2 + \left(\frac{df}{dn_1}\Delta n_1\right)^2 + \left(\frac{df}{dn_2}\Delta n_2\right)^2}. \tag{2}$$

On the basis of the results reported in Ref. 2, for a radius tolerance of 0.01% and requiring for the focal length a tolerance of 0.1% (as prescribed for precise optics), we obtain that the refractive index fluid, the parameter which mostly influences the focal length of whole instrument (as one can deduced by the analysis of the sensitivity coefficients from Eq. (1)), should not change more than 0.0004. If we hypothesize that the main index variations are due to the thermal changes, this means that, during activity, the fluid temperature should not vary more than 1°C.

Now, the telescope will probably be installed in a mountain location on the Alps in Italy. Therefore, it's possible to hypothesize for MezzoCielo a temperature range of [-5,+20]°C, based on the average temperatures registered at the Mount Ekar observation station in Asiago,[5] where is located the largest telescope on the Italian territory. The temperature variation in this thermal range must not produce an alteration of the main parameters greater than the uncertainty coming from construction and measurements, in particular, as seen above, for the fluid refractive index. A solution could consist in keeping constant the fluid temperature between 19 and 20°C employing a

Further author information: (Send correspondence to Silvio Di Rosa)
Silvio Di Rosa.: E-mail: silvio.dirosa@inaf.it, Telephone: +39 331 332 5502

re-circulation system. Such a system reveals useful since, in this way, it could be possible to exploit the high thermal capacity of the liquid mass in order to warm the entire instrument, avoiding excessive temperature differences between its several components.
As a case study, we can suppose that the telescope is continuously employed for 8 hours at the (constant) outer temperature of T_e=-5°C in a natural convection regime (namely, the wind effects are not considered). We are interested in estimating the temperature drop the lenses are subjected to.
Considering a constant (room) temperature for the fluid, it's possible to write a thermal balance equation for the entire telescope:

$$(Mc_p)_g \frac{dT}{dt} = \frac{T_0 - T}{R_{th,g}} - h_{conv}\pi D^2 (T - T_e). \tag{3}$$

In Eq. (3), M represents the glass shell mass, c_p the BK7 specific heat, $R_{th,g}$ the thermal resistance of the spherical glass shell, t time, D the telescope diameter, while T the telescope outer surface temperature. The convective coefficient h_{conv} is, instead, computed employing the heat transfer theory applied to a sphere immersed in quiet air, therefore in natural convection regime. Solving Eq. (3), the time law ruling the variation of T is obtained:

$$T(t) = (T_0 - T_p)\exp(-\frac{t}{\tau}) + T_p, \tag{4}$$

being τ the instrument thermal constant and T_p the steady-state temperature. Since $\tau \approx 20\ 000$ s and $T_p \approx$ 14.5°C, after 8 hours the lenses outer surface would reach a temperature of around 16°C, namely a temperature difference of 4°C is established across the glass shell. The radius decrease can be approximated by:

$$\Delta R_1 = R_1 \alpha \Delta T, \tag{5}$$

which is about -32 μm. Such value should be added to the maximum displacement the lenses are subjected to due to the gravitational loads in order to estimate the total change in the radius of curvature.

2.1 Frame sizing

We will now focus upon the sizing of the frame supporting the lenses and on the coupling between such elements. The starting point is the frame material choice. The lattice has to provide the required rigidity in order to reduce the lenses displacements, without reaching the yielding strength limit; moreover, its material has to exhibit a Coefficient of Thermal Expansion (CTE) similar to the BK7 one in order to minimize thermal stresses, has to be compatible with fluorine fluids, affordable and feasible in large quantities. Such characteristics lead to the choice of metallic material. Among them, it has been selected Kovar, a iron-nickel-cobalt alloy, which exhibits the same elasticity, strength and possibility of mass production of steel, but with a CTE significantly lesser.
The sizing of the Kovar frame is based on the geometry of the dodecahedral structure and on mechanical considerations. The lattice is conceived as a sequence of L-shape beams arranged along the edges of the Platonic solid; their flanges are in contact with the fluid. In order to minimize their deflections, allowing at the same time a good interface between lenses and frame, it's chosen to consider 20 mm wide, 10 mm thick flanges. From construction science, such dimensions should ensure a flange deflection less than 2 μm. The 1000 mm clear aperture of the lenses is therefore surrounded by the frame flanges. The height of the L-shape beam is constrained by the overall geometry: to allow a clear aperture of 1000 mm and to realize a dodecahedral lattice fitting exactly within a 1120 mm radius sphere, the frame L-beams should be no more than 45 mm high, with webs of 35 mm. Eventually, in order to improve the quality of the coupling frame-lenses in terms of displacements, a 10 degrees taper angle is foreseen. Such considerations apply for a frame supporting lenses of both pentagonal and circular shape, with the only difference that, for circular lenses, the frame covers an area around 2.3 times greater than that requested for pentagonal shape lenses.
Regarding the lens geometry, the outer radius has to be 1120 mm, with thickness of 120 mm and 1000 mm clear aperture. The contact with the frame will take place along the entire length of the frame's webs and flanges. For both lenses types, sharp edges should be smoothed out creating chambers: it's immediate to observe that such operation is much more critical for the pentagonal lens, which requires, in addition to those of the circular lens, also the beveling of all the 5 sharp corners in order to avoid stress concentrations. The size of the beveling

has been firstly chosen arbitrarily and then, after several finite element simulations, it has been selected the one assuring minimum stress. The lenses lateral sides exhibit a 10 degrees taper angle. The front view of the single lens assembly described up to this point is depicted in Fig. 2 for both pentagonal and circular shape.

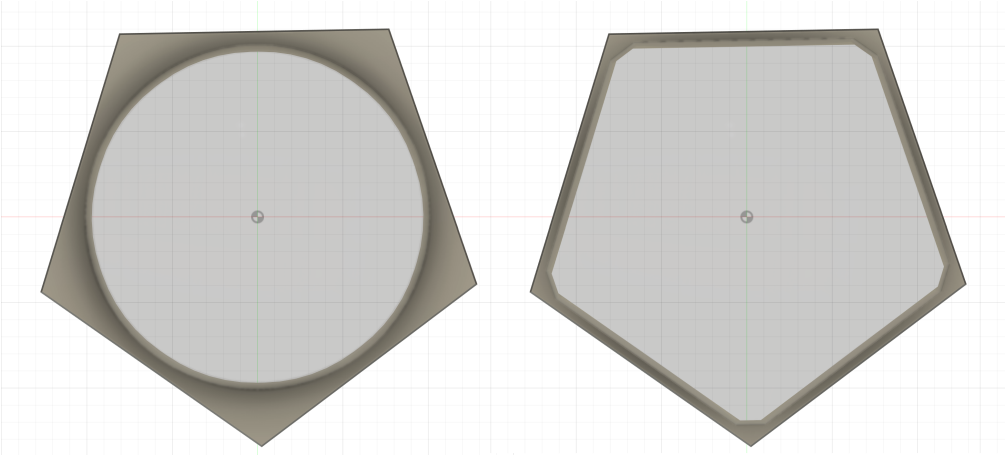

(a) (b)

Figure 2. Front view of the MezzoCielo lens assembly: (a) circular lens, (b) pentagonal lens

In terms of thermal design, it is desirable that the metallic frame temperature exhibits the same variation law of the glass shell one. The values of τ and T_p in Eq. (3) have hence been used to estimate the required frame thermal resistance. After some calculations, we found that, in order for the frame to show a thermal gradient similar to the glass one, it has to be covered with an insulating material having thermal conductivity of around 0.025 W m^{-1} K^{-1}: a polyurethane layer 7.5 mm thick for the pentagonal shape lens and 5 mm thick for the circular one should assure the required thermal balance. The equivalent thermal resistance given by the frame and lenses ones, arranged parallel to each other, is consistent with the glass shell total resistance employed in Eq. (3).
Finally, regarding the coupling between lenses and frame, it is chosen to employ adhesive bounding. For the side bounding, the one bearing the most load, the two components epoxy Milbond is employed as structural adhesive. The axial joint, instead, has to provide primarily the watertightness of the system, therefore it must not chemically react with the fluid, along with a reasonable degree of rigidity and strength. A suitable choice could be represented by the Scotch-Weld Epoxy Adhesive 2214 Regular, a one part epoxy produced by 3M Company, which combines high rigidity, strength and sealing properties.
A first sizing of the adhesive layers could be done in terms of athermalization. Indeed, as suggested by Ref. 6, if the bounding layer has a particular thickness, the assembly will, to a first-order approximation, be athermal in the radial and axial direction. This thickness can be computed with:

$$t_a = l\frac{(1-\nu_e)(CTE_m - CTE_g)}{CTE_a - CTE_m - \nu_e(CTE_g - CTE_a)}. \tag{6}$$

In Eq. (6), the pedices a, m, g refer respectively to adhesive, metal and glass. With Eq. (6), we can compute the structural adhesive thickness substituting to the length l the lens radius and the sealant thickness if $l = t$, being t the lens thickness. In Tab. 1, the materials taken into account for the several components of the telescope assembly are listed along with their main properties, namely Young's module E, tensile, yield and shear strength for glass, metal and adhesives respectively, thermal conductivity k and CTE.

Table 1. Telescope assembly materials main properties

	Material	E (MPa)	Strength (MPa)	k (W m^{-1} K^{-1})	CTE (K^{-1})
Lenses	BK7	82 000	48	1.2	$7.1{\cdot}10^{-6}$
Frame	Kovar	138 000	345	17	$6.5{\cdot}10^{-6}$
Adhesive	Milbond epoxy	592	17.7	1.36	$62{\cdot}10^{-6}$
Sealant	2214 reg. epoxy	5170	20.7	0.4	$49{\cdot}10^{-6}$
Insulating	Polyurethane	/	/	0.025	/

Defined geometry, materials and thermo-mechanical loads, finite element analysis of the pentagonal and circular assemblies have been performed in order to verify the analytical results.

3. RESULTS

In this section, the main results of the finite element analysis are presented. The simulations have been carried out for all the 12 lenses of the assembly (considered with shape both circular and pentagonal), but here, for brevity, only those regarding the most loaded lens, the lowermost one, are shown.
The first result is presented in terms of temperature. In Fig. 3, the outer surface of the lens assembly is depicted for both pentagonal and circular glass elements.

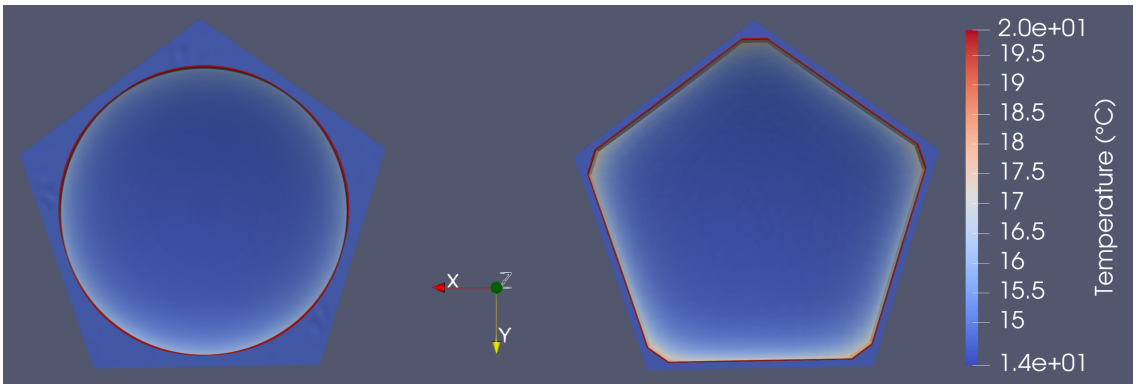

(a) (b)

Figure 3. Temperature distributions upon the outer surface of the lenses assembly: (a) circular lens, (b) pentagonal lens

The temperature distributions in Fig. 3 have been achieved considering a steady-state situation, characterized by a (constant) outer temperature of -5°C in natural convection regime and assemblies inner surface at the constant temperature of 20°C (not shown in Fig. 3). The numerical results confirm that, regardless of the lens shape, the lowest temperature reached by the optical device is around 14°C and, above all, that such temperature is the same for both frame and glass components.
Regarding the safety factors, the latter are computed using the following formula:

$$SF = \frac{\sigma_u}{\sigma_{max}}, \tag{7}$$

where σ_u represents the ultimate stress, namely the material yield or the tensile strength, while σ_{max} is the maximum stress which occurs in the component as a consequence of the applied loads. The latter is computed in terms of Von Mises stress for the metallic frame and maximum principal stress for glass and adhesives. In Fig. 4, it's reported the safety factors distribution for the lowermost lens, subjected, in addition to its own weight, to the highest hydrostatic pressure and to the thermal loads descending from the configuration described

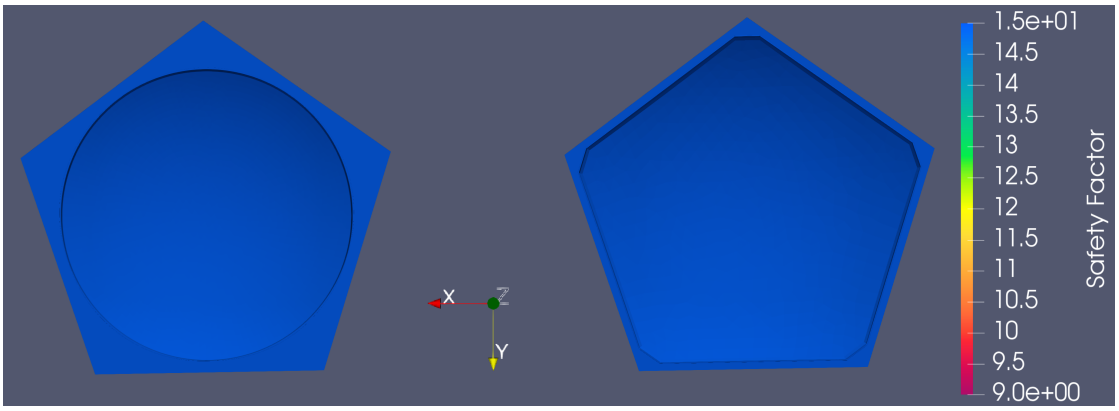

(a) (b)

Figure 4. Safety factors distribution for the lenses assembly. The FEA take into account a fixed constraint for the pentagonal frame edges: (a) circular lens, (b) pentagonal lens

in Fig. 3. Safety factors everywhere higher than 14 assure the design reliability and provide a promising result in the context of the telescope actual realization.
The distribution of displacements in the direction parallel to the optical axis one (Z axis) is, instead, shown in Fig. 5 for both the lenses types. Loads and constraints are those described above for the safety factors simulation: a temperature difference of about 6°C across each assembly, gravitational loads and fixed frame edges are therefore the boundary conditions of the analysis.

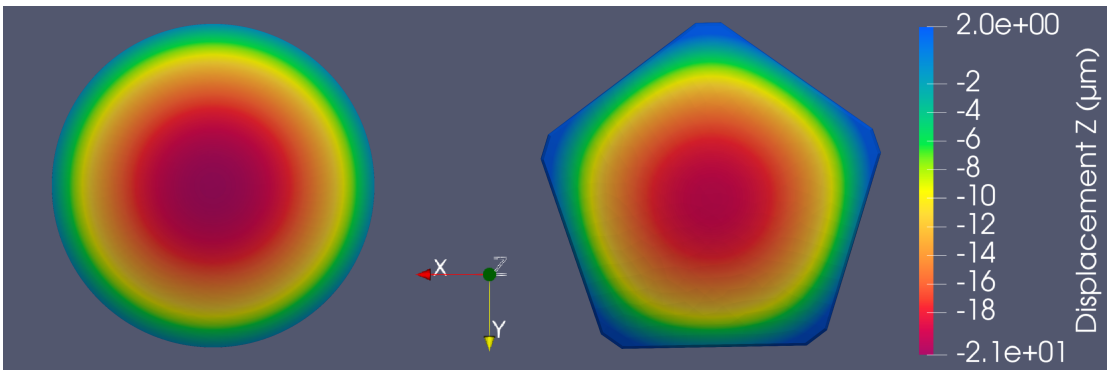

(a) (b)

Figure 5. Z displacements of the lowermost lens subjected to thermal and gravitational loads. The positive sign denotes outwards displacements, the negative one inwards displacements. The lenses are enclosed in the metal frame and bonded using adhesives (not shown in figure): (a) circular lens, (b) pentagonal lens

In Fig. 5, the lenses displacements are computed considering the glass elements bonded to the metallic frame, which is not shown. A comparison between the two lenses suggests that, given the same load and constraint conditions, the pentagonal lens displaces less than the circular one: the maximum displacement (computed with respect to the ideal spherical geometry of an unloaded lens) is around 21 and 19 μm for the circular and pentagonal lens respectively. This happens probably as a consequence of the pentagonal supports arrangement, which tends to keep unchanged the lens position, minimizing the related deformation. The related curvature radius change is not greater than 170 μm, lesser or comparable with the tolerance for precise optics.

4. BIREFRINGENCE ANALYSIS

In this section, the birefringence analysis of the MezzoCielo glass elements is performed.
The birefringence phenomenon happens when the refractive index of a glass, normally isotropic, becomes locally anisotropic due to the presence of stress. This means that along the directions parallel and perpendicular to that of the stress is established a difference in the values of n, which, in turn, produces phase retardation and optical path difference proportionally to the stress itself.[7]
Goal of the study is the quantification of birefringence in terms of refractive index change along the principal stress directions and phase retardation. The birefringence analysis follows the procedure employed in Ref. 8. From the FEA executed in *Fusion360*, the stress tensor for each node of each lens has been estimated:

$$StressTensor = \begin{pmatrix} \sigma_x & \tau_{xy} & \tau_{xz} \\ \tau_{yx} & \sigma_y & \tau_{yz} \\ \tau_{zx} & \tau_{zy} & \sigma_z \end{pmatrix}, \tag{8}$$

where σ and τ represent the normal and shear stresses respectively, computed in a coordinate system XYZ with the Z axis parallel to the lens optical axis and directed outward and the lens lying in the XY plane. For each stress state, one can identify a mutual orthogonal system in which the shear stresses are zero, acting only the normal components of stress. The latter are called principal stresses and they act along principal directions, normal to the principal planes.
The stress tensor and corresponding principal stresses and directions have hence been estimated for each lens of the assembly, considering both gravitational and thermal loads acting. In particular, it has been verified that the third principal direction is parallel to the sphere normal. Therefore, at least in a first approximation, we can compute the amount of birefringence as:

$$\Delta n = k_g(\sigma_1 - \sigma_2), \tag{9}$$

where σ_1 and σ_2 are the first and second principal stresses whose directions lie in the plane perpendicular to the sphere normal, while k_g is the glass stress-optical coefficient, function of wavelength, glass type and temperature. For BK7, at the ambient temperature of 20°C and in the visible range, $k_g = 2.76{\cdot}10^{-6}$ mm^2/N. When light propagates through a birefringent material with birefringence of Δn and thickness t, the corresponding phase retardation δ can be estimated as:

$$\delta = \frac{2\pi}{\lambda}(\Delta n)t. \tag{10}$$

The first, second and third principal stresses distributions for the telescope lowermost lens are described in Figs. 6, 7 and 8 respectively for both pentagonal and circular shape lenses. The boundary conditions are the ones described above in the context of the safety factors analysis. The birefringence and phase retardation distributions are reported in Figs. 9 and 10 respectively for glass thickness of 120 mm and $\lambda = 580.7$ nm.

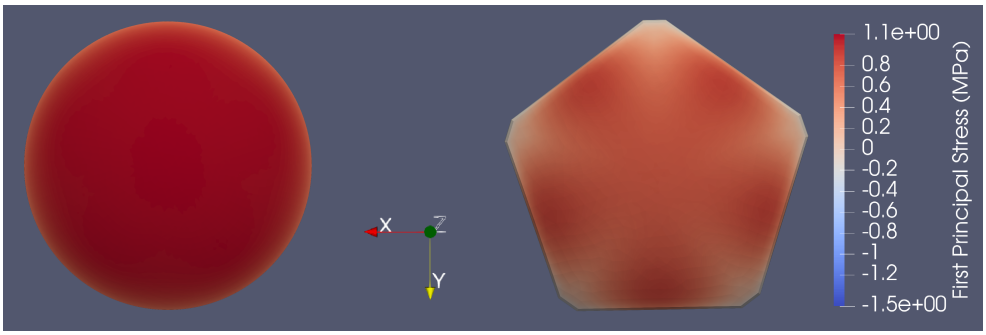

(a) (b)

Figure 6. First principal stress distribution for the lowermost lens subjected to thermal and gravitational loads: (a) circular lens, (b) pentagonal lens

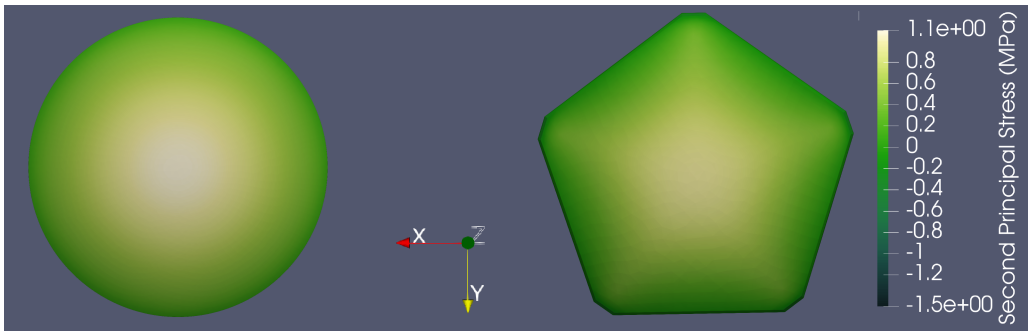

(a) (b)

Figure 7. Second principal stress distribution for the lowermost lens subjected to thermal and gravitational loads: (a) circular lens, (b) pentagonal lens

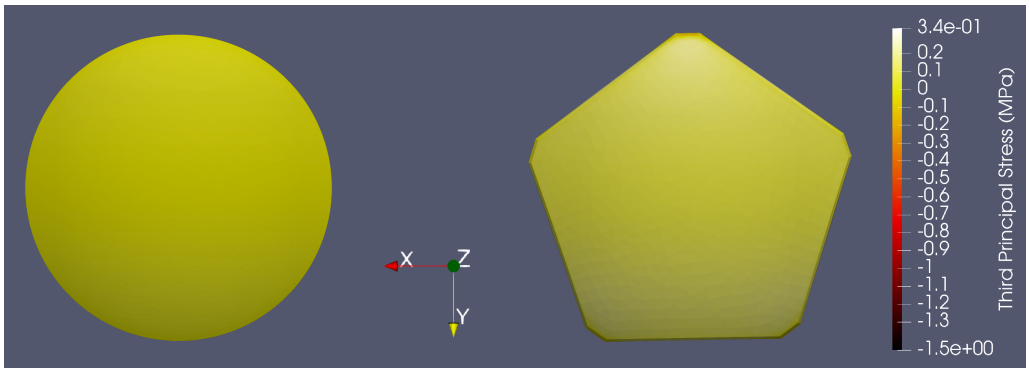

(a) (b)

Figure 8. Third principal stress distribution for the lowermost lens subjected to thermal and gravitational loads: (a) circular lens, (b) pentagonal lens

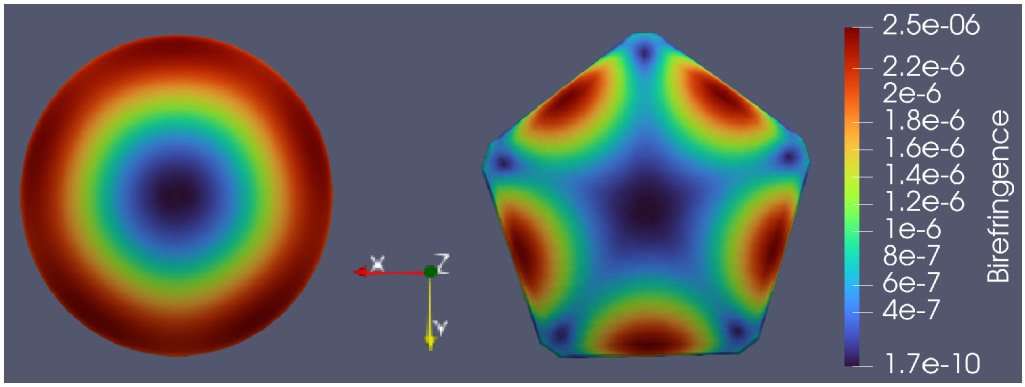

(a) (b)

Figure 9. Refractive index difference between the first and second principal directions for the lowermost lens: (a) circular lens, (b) pentagonal lens

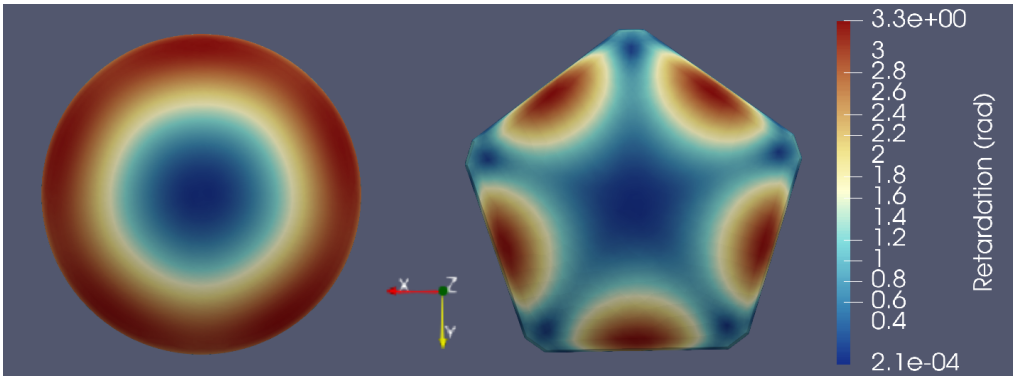

(a) (b)

Figure 10. Phase retardation (in rad) between the first and second principal directions for the lowermost lens: (a) circular lens, (b) pentagonal lens

In Tabs. 2 and 3, instead, a summary of the maximum values of principal stresses, refractive index difference and phase retardation is reported for all the lenses of the assembly, both pentagonal and circular in shape, as well.

Table 2. Principal stresses, refractive index difference and phase retardation max values for the circular lenses at T=-5°C

Lens type	$\sigma_{1,max}$ (MPa)	$\sigma_{2,max}$ (MPa)	$\sigma_{3,max}$ (MPa)	Δn ($\cdot 10^{-6}$)	δ (rad)
Uppermost	0.99	0.63	0.13	2.2	2.7
Upper hemisphere	1.0	0.65	0.13	2.1	2.5
Lower hemisphere	1.1	0.81	0.25	2.6	3.3
Lowermost	1.1	1.0	0.25	2.6	3.3

Table 3. Principal stresses, refractive index difference and phase retardation max values for the pentagonal lenses at T=-5°C

Lens type	$\sigma_{1,max}$ (MPa)	$\sigma_{2,max}$ (MPa)	$\sigma_{3,max}$ (MPa)	Δn ($\cdot 10^{-6}$)	δ (rad)
Uppermost	0.65	0.45	0.22	2.6	3.3
Upper hemisphere	0.66	0.47	0.26	2.6	3.3
Lower hemisphere	0.77	0.65	0.43	2.6	3.3
Lowermost	0.87	0.86	0.34	2.6	3.3

As we can see, birefringence and phase difference increase passing from the lens center to the edges, as a consequence of the fact that the first principal stress values are the highest in these regions and the second principal ones the lowest. The related optical path difference goes from 0 to around $\lambda/2$ passing from the lenses center to the edges.
Moreover, the birefringence, proportional to the difference between the first and second principal stresses, results always positive: this means that the refractive index along the first principal direction is greater than that parallel to the second principal one, and the latter therefore represents the propagation fast axis. On the basis of the Mueller theory,[9] which provides the most general description of the interaction between light and optical elements in terms of polarization, each lens can be seen as a wave-plate, namely as a phase retarder which can be considered linear (at least in a first approximation); we can state that the lenses central portion behaves like an attenuation

filter, characterized by little retardation, while, departing from the center, the phase difference starts to increase, the polarization becomes elliptical (0.1 rad $< \delta <$ 1.57 rad), then changing to purely circular polarization ($\pi/2$ rad phase difference), hence to elliptical and eventually linear polarization again, but perpendicular to the central polarization (π rad phase retardation) along the lenses edges. The latter birefringence state concerns the entire perimeter of the circular lens, and a limited portion of the 5 edges for the pentagonal one. Furthermore, the numerical computations demonstrate that the fast axis angle (comprises between the second principal direction and the X axis) varies between $\pi/2$ rad (at the center) and $3/4\pi$ rad (at the edges).

5. CONCLUSIONS

In this paper, the thermo-mechanical sizing of the MezzoCielo structure has been described.
The (supposed) environmental conditions during the winter activity have been chosen to size the telescope frame with the dual objective of keeping constant (within the tolerances) the telescope focal length and to minimize the thermal gradients between the instrument components (glass optics, metallic frame and adhesives). Indeed, several finite element analysis have shown that the combination of both thermal and mechanical loads is much more severe, in terms of stresses, with respect to the only gravitational ones: safety factors, stresses and strains have been therefore estimated in such worst-case scenario. The results are promising since they confirm the frame robustness and rigidity.
Eventually, the principal stresses within the lenses (both circular and pentagonal in shape) have been estimated and employed to compute the amount of birefringence in terms of refractive index difference and phase retardation. The result was the achievement of a retardation map for each lens of the assembly: the phase difference is comprised between 0 and $\lambda/2$ for the single lens. Moreover, the amount of birefringence allows us to classify the glass elements under analysis as employable for astronomical purposes (based on the Schott suggestions[10]).
Summarizing, it has been verified that the pentagonal lenses exhibit a lesser amount of displacements and stresses with respect to the circular ones, given the same boundary conditions; moreover, their birefringence is located mainly in a limited area around the edges, while the circular lenses birefringence occupies a significant portion of the clear aperture; finally, employing pentagonal lenses would allow reducing the obstruction produced by the metallic frame, for the benefit of the amount of gathered light and, therefore, limiting magnitude of the observable objects and resolution.
These advantages are counterbalanced by the increased manufacturing complexity and cost related to the realization of pentagonal lenses respect to "more standard" circular ones.
The final decision regarding the MezzoCielo lenses shape should be made after the execution of tests on optical and mechanical bench, prepared in order to validate the results presented in this work.

REFERENCES

[1] Ragazzoni, R., DiRosa, S., Dima, M., Arcidiacono, C., Cerpelloni, P., Farinato, J., Magrin, D., and Zaggia, S., "Current status of mezzocielo: a design aiming to a large aperture, extremely wide field of view telescope," in [*Ground-based and Airborne Telescopes IX*], *Proc. SPIE* **121820H** (Aug. 2022). [doi:10.1117/12.2629877].

[2] DiRosa, S., Ragazzoni, R., Pelizzo, M. G., Corso, A. J., Santi, G., Arcidiacono, C., Magrin, D., and Dima, M., "Fluorine fluids experimental determination of the refractive index spectral and thermal variation and transparency quantification for mezzocielo telescope," in [*Advances in Optical and Mechanical Technologies for Telescopes and Instrumentation VI*], *Proc. SPIE* (2024).

[3] DiRosa, S., Ragazzoni, R., Magrin, D., Arcidiacono, C., Dima, M., Farinato, J., Zaggia, S., and Debei, S., "Finite element analysis of the mezzocielo monocentric optical system and other mechanical issues," in [*Ground-based and Airborne Telescopes IX*], *Proc. SPIE* **121823S**, 78–97 (Aug. 2022). [doi:10.1117/12.2629947].

[4] Timoshenko, S., [*Strength of Materials, Part II, Advanced Theory and Problems*], D. Van Nostrand Company, Princeton, New Jersey, third ed. (1956).

[5] INAF, "Mount ekar observing station." Astronomical Observatory of Padua, https://web.oapd.inaf.it/meteo-ekar/archive.php. (Accessed: May 2024).

[6] Yoder, P. L., [*Opto-Mechanical Systems Design*], CRC Press, Taylor & Francis Group, New York, third ed. (2006).

[7] Born, M. and Wolf, E., [*Principles of Optics*], Cambridge University Press, Cambridge, United Kingdom, seventh ed. (1999).

[8] Anche, R. M., Maharana, S., Ramaprakash, A. N., Khodade, P., Modi, D., Rajarshi, C., Kypriotakis, J. A., Blinov, D., Eriksen, H. K., Ghosh, T., Panopoulou, G. V., Pelgrims, V., Skalidis, R., Pearson, T. J., Gjerløw, E., Mandarakas, N., Pavlidou, V., Potter, S. B., Readhead, A. C. S., Tassis, K., Basyrov, A., Papadaki, K., Svalheim, T. L., and Wehus, I. K., "Stress-induced birefringence in the lenses of wide-area linear optical polarimeter-south," in [*Advances in Optical and Mechanical Technologies for Telescopes and Instrumentation V*], *Proc. SPIE* **12188** (Aug. 2022). [doi:10.1117/12.2629515].

[9] Bass, M., [*Handbook of Optics, Vol. 1: Geometrical and Physical Optics, Polarized Light, Components and Instruments*], McGraw Hill, New York, third ed. (2010).

[10] SCHOTT, "Tie 27: Stress in optical glass." Schott Company, Technical Information Advanced Optics, August 2023, https://www.schott.com/en-th/products/optical-glass-p1000267/downloads.